6. Heat Engine Cycles

Compiled September 22, 2025

Mur Meow[1]

[1]Student ID: —— , Deee
*-----

†This report was prepared using a template adapted from the 'arxiv_two_column' repository, available at https://github.com/myst-templates/arxiv_two_column.

Abstract

The main objective of this experiment was to construct and analyze the Pressure-Volume ($P - V$) diagram for a simple air-based heat engine. The engine was operated through a four-stage thermodynamic cycle using two different masses (200g and 400g), with two runs performed for each mass. The experimental efficiencies were calculated and compared to the theoretical maximum Carnot efficiency. For the 200g mass runs, an average actual efficiency of approximately 0.6% was measured against a theoretical maximum of 10%. For the 400g mass runs, the average efficiency was approximately 1.1% against a theoretical maximum of 14%. The most significant finding was that the propagated uncertainty for the net work and efficiency was one to two orders of magnitude larger than the measured values themselves. This result indicates that the engine's net work output is statistically indistinguishable from zero due to fundamental limitations in the precision of the volume measurement system.

1 Introduction

A heat engine is a device that converts thermal energy into mechanical work by operating according to a thermodynamic cycle. The purpose of this experiment is to study the principles of a heat engine in practice by constructing and analyzing a four-stage thermodynamic cycle using a simple system of a piston and cylinder filled with air. The main tasks are to construct a $P - V$ diagram for the cycle, calculate the net work done, determine the heat absorbed from the hot reservoir, and calculate the actual efficiency. The experimental efficiency is then compared with the maximum theoretical efficiency specified by the Carnot cycle for the same operating temperatures, which allows for a quantitative analysis of the engine characteristics and limitations of the experimental method.

2 Theoretical Background

A heat engine is a device that does work by extracting thermal energy from a hot reservoir and exhausting thermal energy to a cold reservoir. In this experiment, the heat engine consists of air inside a cylinder that expands when an attached can is immersed in hot water. The expanding air pushes on a piston and does work by lifting a weight. The heat engine cycle is completed by immersing the can in cold water, which returns the air pressure and volume to the starting values.

The efficiency of a heat engine can be generally expressed as the ratio of output work to input heat[1]:

$$e = \frac{\text{output}}{\text{input}} = \frac{W}{Q_H} = \frac{Q_H - Q_C}{Q_H} = 1 - \frac{Q_C}{Q_H} \tag{1}$$

By the 2nd law of thermodynamics, $\Delta S_C - \Delta S_H \geq 0$, which implies that the efficiency has an upper limit defined by the Carnot cycle efficiency:

$$e \leq 1 - \frac{T_C}{T_H} \tag{2}$$

At the beginning of the cycle, the air is held at a constant temperature while a weight is placed on top of the piston. Work is done on the gas, and heat is exhausted to the cold reservoir. The internal energy of the gas ($\Delta U = nC_v\Delta T$) does not change, as the temperature does not change. According to the First Law of Thermodynamics, $\Delta U = Q - W$, where Q is the heat added to the gas and W is the work done by the gas.

In the second part of the cycle, heat is added to the gas, causing the gas to expand, pushing the piston up, and doing work by lifting the weight. This process takes place at constant pressure (atmospheric pressure) because the piston is free to move. For an isobaric process, the heat added to the gas is $Q_p = nC_p\Delta T$, where n is the number of moles of gas in the container, C_p is the molar heat capacity for constant pressure, and ΔT is the change in temperature. As air consists mostly of diatomic molecules, $C_V = 5R/2$ and $C_p = 7R/2$.

In the third part of the cycle, the weight is lifted off the piston while the gas is held at the hotter temperature. Heat is added to the gas and the gas expands, doing work. During this isothermal process, the work done is given by

$$W = nRT \ln\left(\frac{V_f}{V_i}\right) \tag{3}$$

where V_i is the initial volume at the beginning of the isothermal process and V_f is the final volume at the end of the isothermal process. Given that the change in internal energy is zero for an isothermal process, the First Law of Thermodynamics shows that the heat added to the gas is equal to the work done by the gas:

$$\Delta U = Q - W = 0 \tag{4}$$

In the final part of the cycle, heat is exhausted from the gas to the cold reservoir, returning the piston to its original position. This process is isobaric and the same equations apply as in the second part of the cycle[2].

For specific processes within our cycle:

- **For an isobaric process** ($\Delta P = 0$), the work done is $W = P(V_C - V_B) = nR(T_C - T_B)$. The heat added is $Q = \Delta U + W$. For a diatomic molecule ($C_P = \frac{7}{2}R$), this becomes $Q = \frac{5}{2}nR(T_C - T_B) + nR(T_C - T_B) = nC_P\Delta T$.
- **For an isothermal process**, the heat added is equal to the work done: $W = Q = nRT \ln(V_f/V_i)$.

These relationships are derived from the ideal gas law, $PV = nRT$, and the first law of thermodynamics, $\Delta U = Q - W$.

Based on the principles above, the following specific formulae were used to analyze the experimental data.

Net Work (W) The net work, corresponding to the area of the $P - V$ cycle, was calculated using the shoelace formula for the four vertices $(V_A, P_A), \ldots, (V_D, P_D)$:

$$W = \frac{1}{2}\Big|(V_A P_B + V_B P_C + V_C P_D + V_D P_A) - (P_A V_B + P_B V_C + P_C V_D + P_D V_A)\Big| \tag{5}$$

Absorbed Heat (Q_H) The total heat absorbed, Q_H, is the sum of the heat added during the isobaric ($B \to C$) and isothermal ($C \to D$) expansions. The heat for the isobaric process $B \to C$ was calculated as:

$$Q_{B\to C} = \frac{7}{2}P_B(V_C - V_B) \tag{6}$$

The heat for the isothermal process $C \to D$ was calculated as:

$$Q_{C\to D} = P_D V_D \ln\left(\frac{V_D}{V_C}\right) \tag{7}$$

3 Methods

The raw data and sample scatter plots are available on Google Drive[**?**].

3.1 Apparatus

The software continuously recorded the pressure and position of the piston, creating a $P - V$ diagram for the completed cycle.

The equipment used during the experiments is listed below:

- Heat engine. A device consisting of a cylinder with a piston and fasteners.
- Sensors: Low Pressure Sensor, Rotary Motion Sensor (for measuring the position of the piston), Temperature Sensors.
- Rod and stand.
- Metal can with a tube.
- Two flasks with cold and hot water.
- Thread.
- 2 weights of 200 g each.
- Caliper and ruler.
- Computer equipment for connecting sensors.
- DataStudio software for data collection and analysis.

3.2 Procedure

The experiment was conducted by passing air (working fluid) through a thermodynamic cycle in a heat engine. A container of cold water served as a refrigerator, and a container of hot water served as a heater. Before recording the data, the system was assembled, and the sensors were connected and tested. Test cycles were conducted before data collection began. The cycle was performed with minimal delays between stages to minimize heat loss to the environment. However, in each stage, thermal equilibrium was achieved by observing changes in pressure and temperature over time.

Figure 1: Experimental setup for the experiment[2].

The cycle began at point A, when the aluminum can was partially immersed in a container of cold water. The following steps were then performed in sequence:

1. **Process $A \to B$ (isothermal compression):** Data recording began. The mass was carefully placed on the piston platform, taking care not to touch the thread thrown over the Rotary Motion Sensor, which led to the compression of the gas at an almost constant low temperature.
2. **Process $B \to C$ (isobaric expansion):** The can was quickly removed from the cold water container and immersed in hot water. The increase in temperature caused the air to expand at nearly constant pressure, raising the piston and mass.
3. **Process $C \to D$ (isothermal expansion):** While the can remained in the hot water container, the mass was

removed from the piston platform, allowing the gas to expand further at an almost constant high temperature.

4. **Process $D \to A$ (isobaric compression):** Finally, the can was transferred from the hot water back to the cold water. The gas cooled and contracted at constant pressure, returning the piston to its approximate initial position, thus completing the cycle.

The software continuously recorded the pressure and position of the piston, creating a $P - V$ diagram for the completed cycle.

3.3 Data Analysis and Error Treatment

The initial data, consisting of pressure, piston position, temperature, and time readings, were processed to construct a pressure-volume ($P-V$) diagram for one engine cycle. The coordinates of the four corner points of the cycle (A, B, C, D) were determined based on this data set. For each corner of the $P - V$ diagram, a set of quasi-static points was selected from the corner region where the system stabilized. The average value of the pressure and volume measurements determined the coordinates of the point. The standard deviation of these same measurements was then calculated to represent the random uncertainty of pressure (δP_{rand}) and volume (δV_{rand}) for that particular point.

3.3.1 Calculation of Thermodynamic Quantities

Net Work (W) The net work done during the cycle, which corresponds to the area bounded by the cycle graph $P - V$, was calculated using Gauss's formula for area (the chord method) for a polygon defined by four vertices (V_A, P_A), (V_B, P_B), (V_C, P_C), and (V_D, P_D):

$$W = \frac{1}{2}\Big|(V_A P_B + V_B P_C + V_C P_D + V_D P_A) - (P_A V_B + P_B V_C + P_C V_D + P_D V_A)\Big|$$

Absorbed Heat (Q_H) Heat is absorbed during isobaric expansion ($B \to C$) and isothermal expansion ($C \to D$). The total heat absorbed Q_H is the sum of the heat added in these two processes:

$$Q_H = Q_{B\to C} + Q_{C\to D}$$

For the isobaric process, assuming air is a diatomic gas ($C_p = \frac{7}{2}R$) and applying the ideal gas law, the heat absorbed is given by:

$$Q_{B\to C} = \frac{7}{2}\frac{P_D V_D}{T_H}(T_H - T_L)$$

For the isothermal process, the heat absorbed equals the work done by the gas:

$$Q_{C\to D} = P_D V_D \ln\left(\frac{V_D}{V_C}\right)$$

Efficiency (e) The actual efficiency of the engine was calculated as the ratio of the net work done to the total heat absorbed:

$$e = \frac{W}{Q_H}$$

This experimental value was compared with the maximum theoretical efficiency of the engine, determined by temperatures T_H and T_C, as specified in Carnot's efficiency:

$$e_{\text{Carnot}} = 1 - \frac{T_C}{T_H}$$

3.3.2 Uncertainty Propagation

A full analytical propagation of errors is exceptionally complex. This section outlines the formulas used to estimate the uncertainties of the key calculated results.

Primary Uncertainties The total uncertainty for each measured variable was determined by combining its random and instrumental components.

- **Uncertainty in Temperature (δT):** The random uncertainty was determined by the standard deviation of the sensor readings.
- **Uncertainty in Pressure (δP):** The random uncertainty was determined by the standard deviation of the selected data cluster.
- **Uncertainty in Volume (δV):** The total uncertainty in volume is a combination of three distinct components:
  1. **Random uncertainty (δV_{rand}):** Determined by the standard deviation of volume readings in a quasi-static data cluster for each point (A, B, C, D).
  2. **Instrumental uncertainty of the initial volume ($\delta V_{0,\text{instr}}$):** uncertainty obtained from the instrumental accuracy of the devices used to measure the initial physical dimensions of the system.
  3. **Instrumental error in volume change ($\delta(\Delta V)_{\text{instr}}$):** error obtained from the instrumental accuracy of measuring the cross-sectional area of the piston (depends on the piston diameter) and the displacement recorded by the rotational motion sensor.

  The analysis showed that the instrumental components of the volume uncertainty, particularly the uncertainty of the initial volume, were the dominant source of error, significantly larger than the random uncertainty.

Uncertainty of Net Work (δW) The uncertainty of the work was calculated based on the total uncertainties of the coordinates of the four vertices using the "shoelace" formula. The calculation was broken down into intermediate steps. First, the uncertainties of the terms were calculated, for example:

$$\delta(V_A P_B) = \sqrt{(P_B \cdot \delta V_A)^2 + (V_A \cdot \delta P_B)^2}$$

Then they were combined using the rule for sums to find the uncertainty of the two main terms in the "shoelace" formula, T_1 and T_2. Finally, the total uncertainty in the work is given by the formula:

$$\delta W = \frac{1}{2}\sqrt{(\delta T_1)^2 + (\delta T_2)^2}$$

Uncertainty of Absorbed Heat (δQ_H) The total uncertainty in the absorbed heat is the quadrature sum of the uncertainties from the two relevant processes:

$$\delta Q_H = \sqrt{(\delta Q_{B\to C})^2 + (\delta Q_{C\to D})^2}$$

The uncertainty for the isobaric heat transfer, $\delta Q_{B\to C}$, was found by propagating the errors from the variables in its formula:

$$\frac{\delta Q_{B\to C}}{Q_{B\to C}} = \sqrt{\left(\frac{\delta P_B}{P_B}\right)^2 + \left(\frac{\delta(\Delta V_{CB})}{\Delta V_{CB}}\right)^2}$$

For the isothermal part, the propagated uncertainty is:

$$\frac{\delta Q_{C\to D}}{Q_{C\to D}} = \sqrt{\left(\frac{\delta(P_D V_D)}{P_D V_D}\right)^2 + \left(\frac{\delta(\ln(V_D/V_C))}{\ln(V_D/V_C)}\right)^2}$$

Uncertainty of Efficiency (δe) The uncertainty in the actual efficiency was calculated using the standard formula for the propagation of uncertainty for a ratio:

$$\frac{\delta e}{e} = \sqrt{\left(\frac{\delta W}{W}\right)^2 + \left(\frac{\delta Q_H}{Q_H}\right)^2}$$

All data analysis was performed using the OriginLab software package [3].

4 Results

4.1 Primary Instrumental Uncertainties

The analysis of the final results relies on the propagation of uncertainties from the initial measurements. The primary instrumental uncertainties for the equipment used in this experiment are listed in Table 1.

Table 1: Instrumental uncertainties of the measurement equipment.

Parameter	Instrumental Uncertainty
Piston Diameter, d_{ps}	± 0.1 mm
Can Diameter, D_{can}	± 0.01 mm
Can Length, L_{can}	± 1 mm
Pulley Diameter, d_{pul}	± 0.01 mm
Volume of the cylinder, V_c	± 1 ml

4.2 Experimental $P - V$ Cycles

The experiment was conducted for two different masses, 200g and 400g, with two measurement runs performed for each mass. The reservoir temperatures were measured independently for each run, leading to a specific theoretical maximum efficiency for each cycle.

4.2.1 Run 1 (200g Mass)

The reservoir temperatures for this run are presented in Table 2.

Table 2: Reservoir temperatures for Run 1 (200g).

Parameter	Value (K)
Hot Temp, T_H	332.6 ± 1.0
Cold Temp, T_L	299.1 ± 0.1

The corresponding Carnot efficiency is $e_{\text{Carnot}} = 10.09\%$. The $P - V$ coordinates and final results for this run are summarized in Table 3.

Table 3: Data and results for Run 1 (200g).

Point	V ±δV (m^3)	P ±δP (Pa)
A	$(2.2090 \pm 0.0016) \times 10^{-4}$	101335 ± 27
B	$(2.2045 \pm 0.0016) \times 10^{-4}$	103546 ± 52
C	$(2.2154 \pm 0.0016) \times 10^{-4}$	103730 ± 40
D	$(2.2187 \pm 0.0016) \times 10^{-4}$	101338 ± 57
Calculated Quantities		
Work, W (J)	0.0074 ± 0.24	
Heat, Q_H (J)	0.429 ± 1.40	
Efficiency, e (%)	0.56 ± 56	

4.2.2 Run 2 (200g Mass)

The reservoir temperatures for this run are presented in Table 4.

Table 4: Reservoir temperatures for Run 2 (200g).

Parameter	Value (K)
Hot Temp, T_H	332.7 ± 1.1
Cold Temp, T_L	299.2 ± 0.1

The corresponding Carnot efficiency is $e_{\text{Carnot}} = 10.07\%$. The $P - V$ coordinates and final results for this run are summarized in Table 5.

Table 5: Data and results for Run 2 (200g).

Point	V ±δV (m^3)	P ±δP (Pa)
A	$(2.2087 \pm 0.0016) \times 10^{-4}$	101328 ± 24
B	$(2.2050 \pm 0.0016) \times 10^{-4}$	103551 ± 51
C	$(2.2178 \pm 0.0016) \times 10^{-4}$	103786 ± 21
D	$(2.2223 \pm 0.0016) \times 10^{-4}$	101347 ± 46
Calculated Quantities		
Work, W (J)	0.0031 ± 0.54	
Heat, Q_H (J)	0.510 ± 1.40	
Efficiency, e (%)	0.61 ± 47	

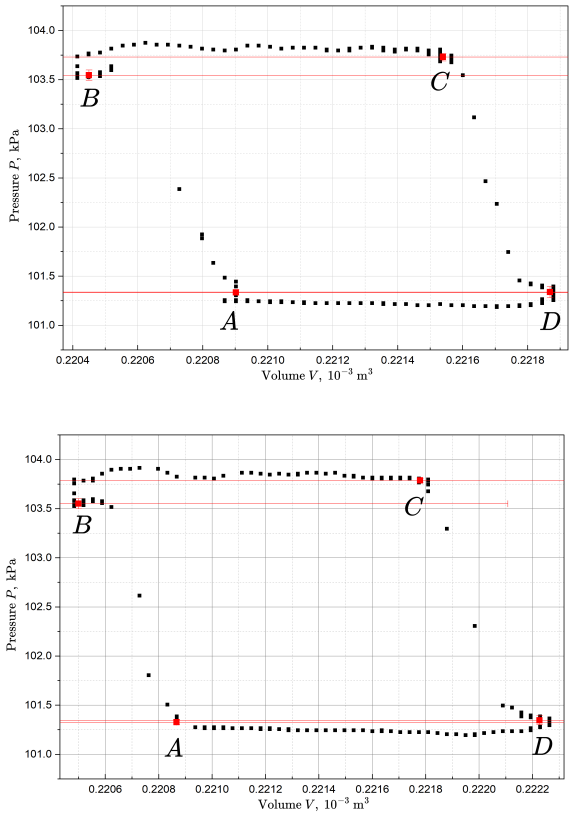

Figure 2: $P - V$ diagrams for the two cycles with the 200g mass, showing Run 1 (top) and Run 2 (bottom).

4.2.3 Run 1 (400g Mass)

The reservoir temperatures for this run are presented in Table 6.

Table 6: Reservoir temperatures for Run 1 (400g).

Parameter	Value (K)
Hot Temp, T_H	348.0 ± 1.4
Cold Temp, T_L	299.4 ± 0.2

The corresponding Carnot efficiency is $e_{\text{Carnot}} = 13.98\%$. The $P - V$ coordinates and final results for this run are summarized in Table 7.

Table 7: Data and results for Run 1 (400g).

Point	V ±δV (m^3)	P ±δP (Pa)
A	$(2.2089 \pm 0.0016) \times 10^{-4}$	101341 ± 47
B	$(2.1989 \pm 0.0016) \times 10^{-4}$	105786 ± 132
C	$(2.2156 \pm 0.0016) \times 10^{-4}$	106176 ± 45
D	$(2.2234 \pm 0.0016) \times 10^{-4}$	101349 ± 39
Calculated Quantities		
Work, W (J)	0.0074 ± 0.24	
Heat, Q_H (J)	0.700 ± 1.43	
Efficiency, e (%)	1.06 ± 36	

4.2.4 Run 2 (400g Mass)

The reservoir temperatures for this run are presented in Table 8.

Table 8: Reservoir temperatures for Run 2 (400g).

Parameter	Value (K)
Hot Temp, T_H	350.3 ± 1.6
Cold Temp, T_L	299.6 ± 0.1

The corresponding Carnot efficiency is $e_{\text{Carnot}} = 14.48\%$. The $P - V$ coordinates and final results for this run are summarized in Table 9.

Table 9: Data and results for Run 2 (400g).

Point	V ±δV (m^3)	P ±δP (Pa)
A	$(2.2086 \pm 0.0016) \times 10^{-4}$	101335 ± 68
B	$(2.2014 \pm 0.0016) \times 10^{-4}$	105831 ± 115
C	$(2.2166 \pm 0.0016) \times 10^{-4}$	106219 ± 43
D	$(2.2263 \pm 0.0016) \times 10^{-4}$	101345 ± 34
Calculated Quantities		
Work, W (J)	0.0079 ± 0.24	
Heat, Q_H (J)	0.664 ± 1.43	
Efficiency, e (%)	1.19 ± 38	

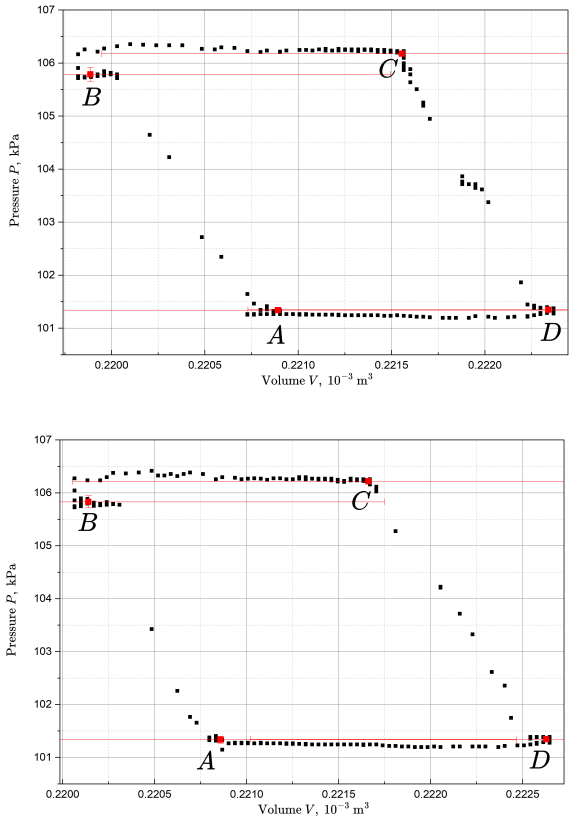

Figure 3: $P - V$ diagrams for the two cycles with the 400g mass.

5 Discussion

5.1 Analysis of Thermodynamic Efficiency and Calculation Method

The experimental efficiency values obtained in this work range from approximately 0.6% to 1.2% and are significantly lower than the theoretical Carnot efficiency values of approximately 11%. This discrepancy is expected due to various irreversible processes occurring in a real engine. However, the decisive factor in obtaining a physically plausible result was the choice of the formula used to calculate the absorbed heat Q_H.

The laboratory manual provided suggests a formula for isobaric heat absorption ($Q_{B\to C}$) based on parameters from another part of the cycle. Although this method is theoretically applicable to an ideal system of ideal gas, it proved to be very sensitive to fluctuations in the values in this experiment. Therefore, a more straightforward formula of the isobaric process was used for the final calculations:

$$Q_{B\to C} = \frac{7}{2} P_B (V_C - V_B) \tag{8}$$

The significance of this choice is substantial. For example, for 200 g, the formula from the manual gives an efficiency of only about 0.056%. In contrast, the direct formula given above gives an efficiency of $\approx$ **0.56%**. The value obtained is almost ten times greater and more consistent with the expected results for this device. This large difference experimentally confirms that the system deviates from the ideal gas model, which makes the direct calculation method more reliable and accurate. Thus, a better model of real gas can be obtained using expressions for Van der Waals gas[4].

In addition, the coordinates of the cycle points (A, B, C, D) were determined by averaging clusters of quasi-static data points directly from the experimental graph. This approach is more accurate than using individual measurements, as averaging minimizes the influence of random errors and outliers.

5.2 Evaluation of Experimental Uncertainty

Despite yielding a more accurate efficiency value, the analysis reveals an exceptionally large associated uncertainty. For all runs, the uncertainty in the calculated efficiency, δe, is significantly larger than the value of e itself. This is not an error in calculation but a fundamental conclusion about the experiment's limitations.

One of the main reasons is the enormous relative uncertainty in the net work (W). Quantitative analysis reveals a critical flaw in the experimental design: the propagated instrumental uncertainty in the measurement of a single volume ($\delta V \approx 1.6 \times 10^{-6}\,\mathrm{m}^3$) is greater than the total net change in volume over the entire cycle (e.g., $\Delta V \approx 1.4 \times 10^{-6}\,\mathrm{m}^3$ for a 200 g cycle). The apparatus attempts to detect a signal that is smaller than its own instrumental noise. As a result, the calculated work is statistically indistinguishable from zero, and its enormous relative uncertainty propagates and dominates the final uncertainty in efficiency.

In addition, the measurement of the initial volume V_0 contributes significantly to the error. Since the error in measuring the volume inside the flask is 1 ml, which is comparable to the amplitude of the volume change of the system in the cycle.

5.3 Model Limitations and Suggestions for Improvement

In addition to measurement uncertainties, the analysis is based on a simplified model with several key assumptions that lead to systematic errors:

- **Assumption of an ideal gas:** In the analysis, air is considered an ideal gas. In reality, air is a real gas, whose behavior is more accurately described by the Van der Waals equation, which takes into account intermolecular forces and the finite volume of molecules.
- **Ignored system volume:** The volume of air in the connecting tube between the tank and the cylinder is ignored in the calculations, although it actively participates in the thermodynamic cycle. However, its value is actually quite small.
- **Imperfect thermal equilibrium:** The model assumes instantaneous and complete heat transfer. In practice, the tank could not be completely immersed in the water tanks, and the water temperature itself fluctuated. In addition, heat was inevitably lost to the environment during transfer.

The most important improvements for this experiment would be:

1) using a more accurate method of measuring volume to reduce the significant uncertainty in the work, and

2) increasing the amount of work done by using a greater temperature difference (e.g., boiling water and an ice bath) to improve the signal-to-noise ratio.

6 Conclusion

During this experiment, we were able to characterize the thermodynamic cycle of a simple heat engine. The efficiency of two configurations was evaluated using masses of 200 g and 400 g. For a mass of 200 g, the average actual efficiency was measured to be $e \approx 0.6\%$, compared to the theoretical Carnot efficiency $e_{\mathrm{Carnot}} \approx 10.1\%$. For a mass of 400 g, the average actual efficiency was $e \approx 1.1\%$, compared to the theoretical maximum $e_{\mathrm{Carnot}} \approx 14.2\%$.

The main conclusion is that the experimental error, primarily due to the low accuracy of volume measurement, is extremely large. It was found that the spread of uncertainty in net work (W) and efficiency (e) exceeds the calculated values by several orders of magnitude. This shows that, within the accuracy limits of this device, the net work produced by the engine is statistically indistinguishable from zero. Thus, the main result is not an accurate measurement of efficiency, but rather a quantitative confirmation of the limitations of the experimental setup.

References

[1] Department of Physics KAIST. Heat engine cycle. https://docs.google.com/presentation/d/11spwrmCQR0Xpt7B7sQXI3-jWG6MfW_qM/edit?usp=sharing&ouid=109530158304160578217&rtpof=true&sd=true, 2025. [Online; accessed 2025-09-20].

[2] Department of Physics. 6. heat engine cycles. In *General Physics Laboratory I*, pages 38–42. KAIST, 2025.

[3] OriginLab. Graphing in originlab 2025 pro. https://www.originlab.com/index.aspx?go=products/origin/graphing, 2025. [Online; accessed 2025-09-20].

[4] Wikipedia. Van der waals equation. https://en.wikipedia.org/wiki/Van_der_Waals_equation, 2025. [Online; accessed: 2025-09-20].